

OPEN

Application of Contrast-Enhanced 3-Dimensional T2-Weighted Volume Isotropic Turbo Spin Echo Acquisition Sequence in the Diagnosis of Prolactin-Secreting Pituitary Microadenomas

Rui Guo, MD,* Yue Wu, PhD,† Guangcheng Guo, MD,* Haiyang Zhou, PhD,‡ Shoutang Liu, MD,§ Zhenwei Yao, PhD,† and Yunping Xiao, MD*

Objective: This study aimed to investigate the value of contrast-enhanced 3-dimensional (3D) T2-weighted (T2W) Volume Isotropic Turbo Spin Echo Acquisition (VISTA) sequence in prolactin-secreting pituitary adenoma diagnosis.

Methods: We enrolled 158 patients with hyperprolactinemia. Coronal dynamic contrast-enhanced (DCE) T1 spin echo and T2W VISTA sequences were performed. The detection of pituitary microadenomas in 3 imaging groups (DCE magnetic resonance imaging [MRI], VISTA, and DCE MRI + VISTA) were compared using McNemar test and χ^2 test.

Results: The DCE MRI + VISTA group detected 28 more pituitary microlesions than DCE MRI alone. Among these, 20 lesions were clearly observed on VISTA images but were negative on DCE MRI. The combined sequences showed higher sensitivity (85.3%) and diagnostic accuracy (89.2%) for adenoma detection than any of the sequences alone ($P < 0.01$). We noted that in 65.7% of the patients with adenoma (46 of 70), a “hypointense rim” was present around the lesion on the VISTA images. Of them, 11 patients underwent surgery. Histopathology confirmed that the “hypointense rim” was a pseudocapsular structure at the edge of the adenoma.

Conclusions: For patients with hyperprolactinemia, the 3D T2W VISTA sequence is an important supplement to DCE MRI, because it could improve the detection rate of pituitary microadenomas.

Key Words: MRI, hyperprolactinemia, pituitary adenoma, volume isotropic turbo spin echo acquisition sequence, dynamic contrast-enhanced MRI

(*J Comput Assist Tomogr* 2022;46: 116–123)

The pituitary secretes large amounts of vasoactive biological metabolites (hormones). A glandular disease could change human physiological functions by disturbing the production of hormones. Hyperprolactinemia is a hypothalamic-pituitary axis reproductive endocrine disorder arising from various causes, and prolactin-secreting adenoma is the most common of them.^{1,2} During medical

treatment or operation, accurately detecting and locating the pituitary lesions could help physicians treat patients with hyperprolactinemia during differential diagnosis of the hyperprolactinemia cause, monitoring drug effect, and guiding surgical planning when adenoma resection is needed.³ However, most prolactin-secreting pituitary adenomas are of approximately 2 to 5 mm (microadenoma) and difficult to detect in conventional magnetic resonance (MR) images. It is crucial to improve imaging reliability and display capability for better clinical decision making when treating patients with hyperprolactinemia.^{4–6} Therefore, the MR imaging (MRI) technology for microlesions in the pituitary should be continuously improved to minimize the diagnostic and treatment uncertainty.

Since the 1980s, dynamic contrast-enhanced (DCE) MRI has been maturely used to detect microlesions in the pituitary gland.^{7,8} The anatomical characteristics of the sella turcica area (air, bone, and soft tissue) lead to heterogeneity of the local magnetic field, a source of susceptibility artifacts.^{9,10} Due to the susceptibility artifacts, the slice thickness on routine MR and DCE imaging is usually of approximately 2 to 3 mm. Studies on spoiled gradient echo (SGE) sequence of pituitary microadenomas have been carried out in recent years.^{11–13} It was reported that the SGE sequence showed higher sensitivity than DCE MRI for detecting pituitary microadenomas. Although the sensitivity varies greatly among studies, it still suggests that 20% to 40% of hormone-secreting pituitary microadenomas are incorrectly identified.^{14,15}

The fast spin echo (FSE) technology from the convergence pulse appeared later than the SGE sequence and facilitated 3-dimensional (3D) volume acquisition. This sequence is called 3D sampling perfection with application-optimized contrasts using different flip angle evolution (SPACE) by Siemens or Volume Isotropic Turbo Spin Echo Acquisition (VISTA) by Philips. Each MRI manufacturer has its unique design in terms of the choice of variable flip angles and refocusing pulses. When based on the turbo spin echo (TSE) sequence, it avoids the susceptibility artifacts of the SGE sequence, whereas the minimum layer thickness can be of less than 1 mm when based on the 3D technique.¹⁶ The different systems were studied in clinical applications,^{17,18} including using the SPACE sequence for pituitary adenoma.^{19,20} However, those previous studies did not obtain the clinical or histological data to confirm their diagnoses. Furthermore, there are currently no reports on using the VISTA sequence to detect hormone-secreting pituitary adenomas. Therefore, we compared DCE MRI, 3D T2-weighted (T2W) VISTA, and their combination to evaluate their detection ability of prolactin-secreting microadenomas.

MATERIALS AND METHODS

The hospital review board reviewed and approved this study. We recruited 176 patients with hyperprolactinemia (157 female and 19 male) from January 2018 to June 2019. Informed consent was obtained from all participants. Serum prolactin at rest was

From the *Department of Radiology, Liuzhou People Hospital, Liuzhou; †Department of Radiology, Huashan Hospital, Shanghai Medical College, Fudan University, Shanghai; and Departments of ‡Endocrinology and §Neurosurgery, Liuzhou People Hospital, Liuzhou, China.

Received for publication April 22, 2021; accepted July 22, 2021.

Correspondence to: Yunping Xiao, MD, Department of Radiology, 8 Wenchang Rd, Liuzhou People Hospital, Liuzhou, Guangxi, China 545006 (e-mail: xyp22133@sina.com).

The authors declare no conflict of interest.

Supported by Special Fund for “New Century One, Ten, Hundred Talents Project of Liuzhou City” to Y.X. and Subject of the National Health Commission of Guangxi Zhuang Autonomous Region (Grant Number Z20180280) to Y.X. R.G. and Y.W. contributed equally to this work and are cofirst authors.

Supplemental digital contents are available for this article. Direct URL citations appear in the printed text and are provided in the HTML and PDF versions of this article on the journal’s Web site (www.jcat.org).

Copyright © 2021 The Author(s). Published by Wolters Kluwer Health, Inc. This is an open-access article distributed under the terms of the Creative Commons Attribution-Non Commercial-No Derivatives License 4.0 (CCBY-NC-ND), where it is permissible to download and share the work provided it is properly cited. The work cannot be changed in any way or used commercially without permission from the journal.

DOI: 10.1097/RCT.0000000000001237

TABLE 1. Magnetic Resonance Imaging Parameters

Parameter	Sagittal T1	Coronal T1	3D-T2W VISTA
TR, ms	635	635	1200
TE, ms	10	10	108
FA, degree	90	90	120
FOV	150 × 150	150 × 150	100 × 84
NEX	4	4	2
Bandwidth	260	260	289
Voxel size	1.3 × 0.9 × 1.25	0.75 × 0.9 × 2.5	0.5 × 0.5 × 0.6
Slice thickness, mm	2	2	1
Echo spacing	9.1	9.1	6
No. slices	9	9	24
Matrix size	68 × 134	68 × 134	200 × 150

FA indicates flip angle; FOV, field of view; NEX, number of excitations; TE, time of echo; TR, time of repetition.

measured twice in all patients, with a 14-day interval between measurements. Hyperprolactinemia was defined as serum prolactin concentration higher than 25 µg/L. If the prolactin level was higher than 100 µg/L, the possibility of prolactin-secreting pituitary adenoma was considered after excluding other secondary causes (clinical positive). A prolactin level of 25 to 100 µg/L was considered as clinical negative. Exclusion criteria were as follows: (1) lesion size greater than 10 mm; (2) patients after sellar surgery; (3) hypophysitis or pituitary infection; (4) pregnancy and lactation; (5) taking a drug known to cause hyperprolactinemia; and (6) other parasellar and stalk lesions.

Magnetic resonance images were acquired with a 3.0 Tesla system (Achieva; Philips) using an 8-channel head coil. Each patient underwent precontrast 2D FSE sagittal and coronal T1 weighted image (T1WI) and T2 weighted image (T2WI) scans (conventional MRI), coronal DCE MRI, and coronal contrast-enhanced 3D T2W VISTA sequence. The imaging parameters are shown in Table 1. Dynamic contrast-enhanced MR scans were performed immediately after a standard dose of gadolinium contrast agent (0.1 mmol/kg) was administered. Subsequently, contrast-enhanced 3D T2W VISTA sequence (scanning time, 4 minutes) and conventional sagittal images were acquired. The total scanning time was approximately 20 minutes.

The patient images were classified into 3 groups according to the different sequence combinations. In group 1, a “conventional pituitary protocol” with DCE sequence was performed. This group included precontrast sagittal and coronal T1WI, coronal T2WI, dynamic coronal T1WI, and postcontrast sagittal T1WI sequences. Group 2 included postcontrast VISTA sequence alone. Group 3 was a combination of groups 1 and 2. Three radiologists with over 10 years of experience independently analyzed the

image data in all 3 groups. Each group was evaluated separately with a 2-week interval between groups. The reading order was group 1, group 2, and then group 3. A chart presenting the reading process is shown in Figure 1. The radiologists evaluated the images to determine whether a definite tumor was present (positive), no apparent tumor (negative), or suspected for the presence of a tumor, indicating equivocal findings such as patchy abnormal signal intensity without a clearly defined lesion or a cystic lesion rather than adenoma. Patients were considered radiologically positive when at least 2 of the 3 radiologists identified an adenoma at the same location. Otherwise, the patients were considered radiologically negative or suspicious cases. The presence of cystic area in the adenoma and cystic lesion in the pituitary was also recorded.

Clinical data were compared with the imaging findings to calculate the sensitivity, specificity, positive predictive value (PPV), negative predictive value (NPV), and diagnostic accuracy of the 3 imaging approaches in detecting pituitary adenomas. McNemar test compared the tumor detection ability between the sequence, and the χ^2 distribution was tested between the groups.

RESULTS

Clinical Data

A total of 176 patients underwent pituitary MR scans. After excluding 7 patients with macroadenomas, 7 after surgery, and 4 with pituitary inflammation, the study included 158 patients (137 female and 21 male; age range, 14–66 years; mean age, 37.21 ± 11.73 years). Among them, 9 patients were younger than 20 years, 123 were 20 to 40 years, and 26 were older than 40 years. Their symptoms included irregular menstruation, amenorrhea, and lactation or sexual dysfunction. Seventy-five patients were clinically positive, and 83 were clinically negative.

Lesion Detection Ability

In group 1 (DCE MRI), 63 of the 158 patients (39.9%) were radiologically positive and 95 (60.1%) radiologically negative or suspected, including 27 false-positive and 39 false-negative diagnoses. In group 2 (T2W VISTA images), 36 patients (22.7%) were radiologically positive and 122 (77.2%) radiologically negative or suspected, including 2 false-positive and 41 false-negative diagnoses. Seventy patients (44.3%) in the combination group were radiologically positive, and 88 (55.7%) were radiologically negative or suspected, including 11 false-positive and 6 false-negative diagnoses. The group 3 (combination group) detected 28 more true-positive microadenomas than group 1 (Table 2). Among them, 20 lesions were negative on DCE MRI but clearly observed on the contrast-enhanced T2W VISTA images. Interestingly, 85% of these lesions (17 of 20) included a cystic component in the adenoma that showed a significant hypersignal intensity on the T2W VISTA images (Figs. 2, 3). The signal intensity features of all sequences in the combination group for the 75 clinically positive patients are shown in Table 3.

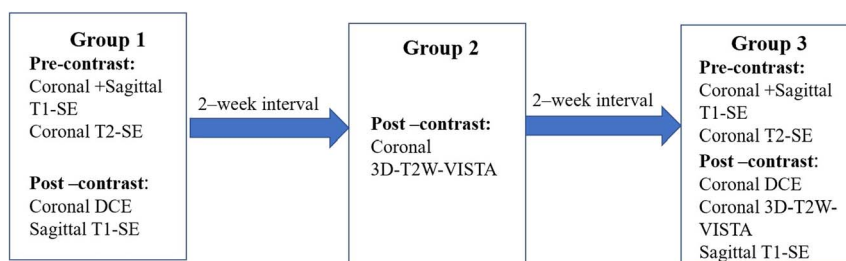


FIGURE 1. The reading process of 3 imaging groups. SE, spin echo.

TABLE 2. Comparative of Imaging and Clinical Results of the 3 MRI Groups

MRI	Clinical Positive	Clinical Negative	Total	Sensitivity	Specificity	PPV	NPV	Diagnostic Accuracy
DCE				48.0%	67.5%	57.1%	58.9%	58.2%
°Positive	36	27	63					
°Negative/suspicious	39	56	95					
°Total	75	83	158					
VISTA				45.3%	97.6%	97.2%	66.4%	72.7%
°Positive	34	2	36					
°Negative/suspicious	41	81	122					
°Total	75	83	158					
DCE + VISTA				85.3%	92.7%	91.4%	87.5%	89.2%
°Positive	64	6	70					
°Negative/suspicious	11	77	88					
°Total	75	83	158					

The combination of DCE MRI and contrast-enhanced 3D T2W VISTA sequence showed a higher sensitivity (85.3%) and diagnostic accuracy (89.2%) for tumor detection. Contrast-enhanced 3D T2W VISTA alone showed high specificity (97.6%) but low sensitivity (45.3%; Table 2). The combination and DCE MRI groups differed significantly in their diagnostic accuracy ($P < 0.01$).

Eleven clinically positive patients underwent transsphenoidal pituitary surgery by the same experienced neurosurgeon. The imaging and surgical findings of these patients are shown in Supplemental Table S1, <http://links.lww.com/RCT/A126>. Nine of the 11

patients were positive on DCE MRI, and 8 of 11 were positive on T2W VISTA. All 11 patients showed distinct lesions in the pituitary before surgery when assessed by the combined sequences. In other words, 2 of 11 patients (18%) benefited from adding the 3D T2W VISTA sequence to demonstrate their lesions. The surgeon located and removed the adenomas during the surgery in all patients. The surgical findings were confirmed by histopathology. Because we had no pathologically negative cases, only the sensitivity of the sequence groups was calculated. The comparative statistics between the groups based on the surgical results are shown in Table 4.

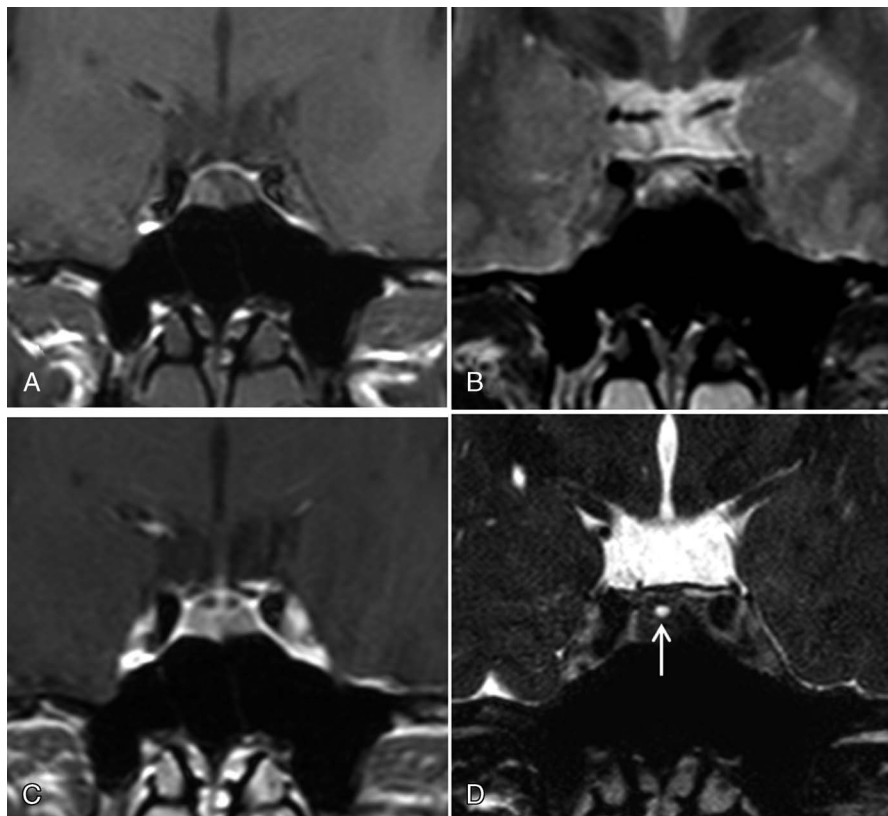


FIGURE 2. A, Coronal pre-enhanced T1WI image. B, Coronal pre-enhanced T2WI image. C, DCE MRI. D, Contrast-enhanced T2W VISTA sequence image. The adenoma is on the right side of the pituitary. The obscure lesion seen on the DCE MRI image (C) is clearly displayed on the contrast-enhanced T2W VISTA sequence image (D).

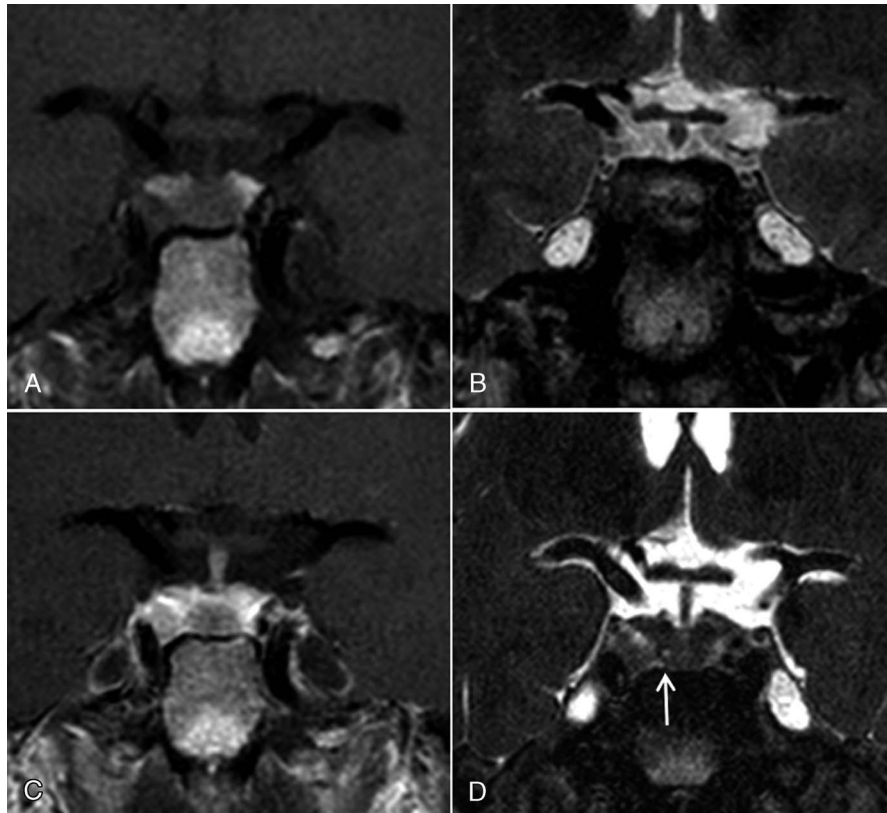


FIGURE 3. A, Coronal pre-enhanced T1WI image. B, Coronal pre-enhanced T2WI image. C, DCE MRI. D, Contrast-enhanced T2W VISTA sequence image. The adenoma is on the right side of the pituitary. No lesion is seen on the DCE MRI image (C), while a lesion is clearly displayed on the contrast-enhanced T2W VISTA sequence image (D).

“Hypointense Rim” Sign Around the Adenomas

We observed a hypointense rim (complete or incomplete) around the lesions of 65.7% of the radiologically positive patients (46 of 70) when assessed on contrast-enhanced 3D T2W VISTA images. Of them, 11 patients underwent surgery. The hypointense rim was histopathologically confirmed as a pseudocapsular structure around the edge of the adenoma. Compressed dense reticular fibers of the pseudo capsule were observed in the histopathological sections, rich in capillary and connective tissue networks in the “rim” area. Only 16.6% of the negative cases (3 of 18) considered as a pituitary cyst rather than adenoma showed hypointense rims on the 3D T2W VISTA images (Figs. 4, 5).

DISCUSSION

We have highlighted in this study the value of contrast-enhanced 3D VISTA sequence for prolactinoma diagnosis. The

combination of 3D VISTA and DCE MRI could detect more pituitary microadenomas than DCE MRI. The diagnostic accuracy of adenoma improved from 58.2% to 89.2% after adding the 3D VISTA sequence. Accurate pituitary microadenoma MRI evaluation could help clinical decision making concerning patients with hyperprolactinemia. Although some studies used transsphenoidal surgery for prolactin-secreting microadenomas,²¹ dopamine agonists are still the first-line treatment for these lesions.^{22,23} Before initiating medical treatment, clear detection of the pituitary lesion on MRI could benefit patients with hyperprolactinemia in several ways: (1) confirmation of prolactinoma diagnosis requires laboratory evidence of sustained hyperprolactinemia and radiographic evidence of a pituitary adenoma. The accurate presentation of a pituitary lesion on the MRI helps in the differential diagnosis of prolactinoma and other nonadenoma hyperprolactinemia causes; (2) distinct lesion manifestation would help monitor drug treatment effects. A decrease in prolactin levels while taking a

TABLE 3. Imaging Features of the 75 Clinical Positive Cases in Combination Group

MRI	DCE		Total	
	Hypoenhancement	Isoenhancement		
3D-T2W VISTA	Hyper(cystic)signal intensity	17 (22.7%)	17 (22.7%)	34 (45.3%)
	Isosignal intensity	23 (30.7%)	11 (14.7%)	34 (45.3%)
	Hyposignal intensity	4 (5.3%)	3 (4.0%)	7 (9.3%)
	Total	44 (58.6%)	31 (41.3%)	75 (100%)

TABLE 4. Comparative of Sensitivity of the 3 MRI Groups in 11 Surgical Patients

MRI	Pathologically Positive	Pathologically Negative	Sensitivity
DCE			81.8%
°Positive	9	0	
°Negative/suspicious	2	0	
°Total	11	0	
VISTA			72.7%
°Positive	8	0	
°Negative/suspicious	3	0	
°Total	11	0	
DCE + VISTA			100%
°Positive	11	0	
°Negative/suspicious	0	0	
°Total	11	0	

dopamine agonist is usually accompanied by considerable tumor shrinkage. Repeated MRI could be performed regularly for continued monitoring.³ Furthermore, it was reported that the heterogeneity of prolactinoma T2 signal during diagnosis might be correlated with the clinical behavior and could be used as a negative predictor of hormonal response to dopamine agonists²⁴; (3) higher confidence in the lesion localization could help surgeons in better surgical planning, avoiding unnecessary pituitary exploration, and enabling a better understanding of the relationship between the tumor and surrounding tissues (eg, cavernous sinus, posterior pituitary, and the pituitary stalk).²⁵

Various modifications of the MRI techniques have been attempted to improve pituitary microadenoma localization. Dynamic contrast-enhanced MRI is already widely used.^{7,8} This

approach refers to the acquisition of MR images within seconds after gadolinium injection. Such images show the best contrast to tell microadenoma from normal pituitary tissue. However, dynamic imaging might generate blurring and technical artifacts that could be interpreted as microadenoma,¹⁰ and approximately 10% to 20% of the general population have nonfunctional pituitary microadenoma or small benign cysts. These could also complicate the differential diagnosis.^{2,26}

Recently, some studies reported the successful use of the T2WI SPACE imaging sequence to diagnose small pituitary gland lesions, improving the detection rate and diagnostic confidence.²⁰ Wang et al¹⁹ found that the T2WI SPACE sequence generated significantly better images than routine MRI in terms of the pituitary gland boundary, definition of pituitary lesions, and overall image quality. VISTA (by Philips) and SPACE (by Siemens) are both TSE 3D sequences, using variable flip angles for refocusing instead of the conventional 180-degree refocusing pulse.^{27,28} Both sequences could offer isotropic thin-section imaging with fewer susceptibility artifacts. Each MRI manufacturer has its unique design characterized by choice of variable flip angles and refocusing pulses. We believe that the results in SPACE studies could be generalized to VISTA. We still focused on detecting pituitary microlesions in this study, but with some experimental design optimizations. The major limitation of the previous studies was that lesion assessments were only based on MRI, without confirmation through the clinical data (hormone level/pathology results). Hence, they only compared the lesion detection rate between T1-SE and SPACE images without diagnose sensitivity and specificity. Furthermore, previous studies included all patients with clinically suspected pituitary abnormalities (hyperprolactinemia, acromegaly, hypogonadism, vision loss, or menstrual disorder), without subdivision for the adenoma type. However, it is well known that different adenoma types could manifest different imaging characteristics on MRI, which might lead to the difference in diagnostic efficacy of pituitary microlesions on T2-SPACE/

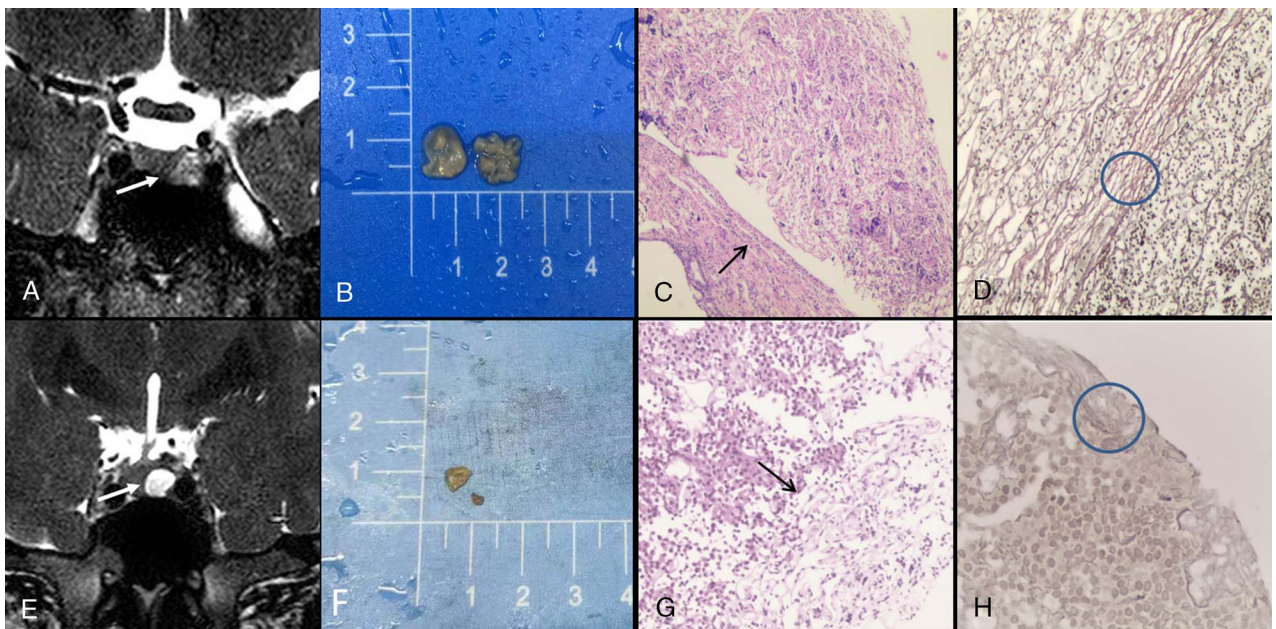


FIGURE 4. Two cases of histopathologically confirmed “hypointense rims” on the VISTA images. A and E, Contrast-enhanced T2W VISTA images. Both tumors were on the left side of the pituitary. The hypointense rim was observed around the tumors (white arrows). B and F, General pathology of pituitary adenoma after surgery. C and G, HE staining of the tumor capsules (black arrows) and adenomas ($\times 40$ magnification). D, Reticular staining of the dense capillary and connective tissue network (circles) in the tumor pseudocapsules around the adenomas ($\times 100$ magnification). HE, hematoxylin and eosin.

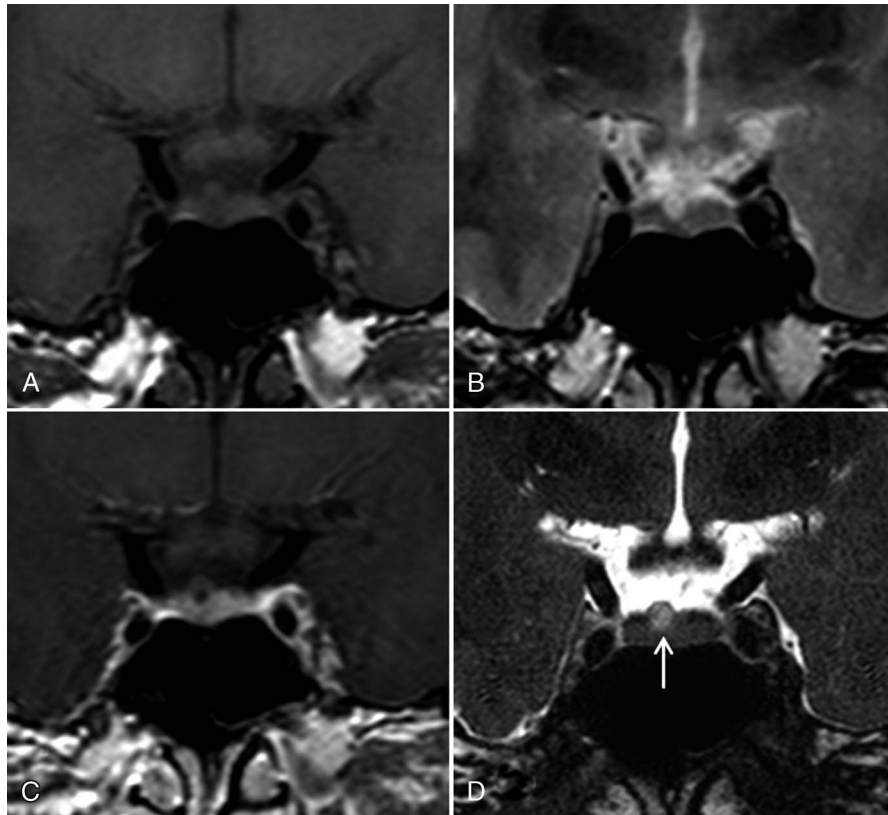


FIGURE 5. A, Coronal pre-enhanced T1WI image. B, Coronal pre-enhanced T2WI image. C, DCE MRI. D, Contrast-enhanced T2W VISTA sequence image. This clinically negative case was diagnosed as having a nontumor lesion (cyst) with an image feature of eccentric bulging (arrow). The lesion did not show the hypointense rim sign.

VISTA images. We focused on prolactinoma, the most prevalent pituitary tumor type. More than 90% of prolactinomas are small, intrasellar tumors. Besides, we combined clinical data with the radiological assessment and used the prolactin level as the standard to determine the sensitivity, specificity, and diagnostic accuracy of the T2W VISTA.

The lesion signal intensity on the T2W VISTA sequence was complex and included low, high, iso-, and mixed-signal intensities. The signal characteristics of T2W VISTA sequence imaging are related to various features of these lesions. Almost half of the prolactinoma lesions (45.3%) in our study showed hypersignal intensity or contained a cystic component on the VISTA sequence. Very few of them (9.3%) showed a hyposignal intensity. The VISTA + DCE MRI sequences in this study detected 28 microadenomas more than DCE MRI. Among them, 20 lesions (85%) showed no significant evidence of adenoma on the DCE MRI but presented a cystic component (significant hypersignal intensity) on the T2W VISTA images. According to the imaging characteristics of contrast-enhanced T2W VISTA, the high-signal signs were not the pituitary adenoma but its cystic part. Because of paramagnetism of the contrast agent, the T1 and T2 relaxation times of normal pituitary tissue and pituitary adenoma were reduced simultaneously in the T2W VISTA sequence.²⁹ A shorter T2 relaxation time means a lower signal intensity of the pituitary tissue. Because the cystic region of the adenoma contains no contrast agent, the effect of shortening the T2 relaxation time cannot be seen in the cystic region. Therefore, the cystic part of the pituitary adenoma shows very good contrast on the contrast-enhanced 3D VISTA images. The hypersignal intensity of adenoma on

VISTA could increase the radiologists' confidence in detecting pituitary microlesions. In some cases, it could be the key diagnostic point. However, 45.3% of the lesions appeared with isointensity, which means that they were radiologically negative on T2W VISTA images. This led to a high rate of false-negative cases in the T2W VISTA sequence alone group. Therefore, pituitary microadenoma diagnosis cannot be achieved by the T2W VISTA sequence alone. Rather, a combination of DCE MRI and contrast-enhanced T2W VISTA sequence is required.

We found in this study that 64.9% of the clinically positive patients showed a hypointense rim (complete or incomplete) around the lesions on the contrast-enhanced T2W VISTA sequence. This rim was absent in nontumor lesions (cysts). Among those with the rim, 8 patients underwent surgery, and the pathological examination confirmed that the lesions were prolactin-secreting pituitary adenomas. The pathological sections showed compressed, dense reticular fibers forming pseudocapsules, rich in capillaries and connective tissue networks, around the edge of the adenomas. Therefore, we speculate that the low linear signal around the tumor was a fibrous pseudocapsular structure. Park et al³⁰ reported that this hypointense rim sign on T2WI was more common with pituitary adenomas than Rathke cleft cysts but provided no pathological explanation. This finding could potentially help differentiate adenomas from cysts. However, the number of pathologically confirmed cases was small, so more studies are needed to confirm it.

Because surgery is not the first line of treatment for prolactin-secreting pituitary adenoma, most cases presented no histological data to confirm the diagnosis. Instead, prolactin level

(100 µg/L) was used as the clinical diagnostic criterion. The magnitude of prolactin elevation can be useful in determining the etiology of hyperprolactinemia because the highest values are observed in patients with prolactinomas.^{31,32} In general, serum prolactin levels parallel adenoma size. Although the number varies in different studies, most patients with prolactin levels over 100 to 150 µg/L (4–5 times higher than the normal values) will have a prolactinoma.^{25,33,34} Macroadenomas are typically associated with levels of over 250 µg/L. Venipuncture stress may cause an elevation in the prolactin level, but it is usually mild (<40–60 µg/L). Most patients with stalk dysfunction, drug-induced hyperprolactinemia, or systemic diseases present with prolactin levels less than 100 µg/L. However, in a few cases, such values are not absolute. Secondary causes of hyperprolactinemia should carefully be ruled out. In addition, further investigations with more pathologic confirmed case and a longer-term follow-up are needed to obtain more accurate data.

One limitation of this study was that we did not include the 3D SGE sequence because of incomplete imaging data in this group of patients. Further study is expected to explore the adenoma detection capacity of a 3D SGE plus VISTA sequence.

CONCLUSIONS

The 3D T2W VISTA sequence is an important supplement to DCE MRI for patients with hyperprolactinemia because the combination could improve the detection rate of pituitary microadenoma.

REFERENCES

- Louis DN, Perry A, Reifenberger G, et al. The 2016 World Health Organization Classification of Tumors of the Central Nervous System: a summary. *Acta Neuropathol*. 2016;131:803–820.
- Singh M, Verma A, Sharma N. Optimized multistable stochastic resonance for the enhancement of pituitary microadenoma in MRI. *IEEE J Biomed Health Inform*. 2018;22:862–873.
- Varlamov EV, Hinojosa-Amaya JM, Fleseriu M. Magnetic resonance imaging in the management of prolactinomas; a review of the evidence. *Pituitary*. 2020;23:16–26.
- Amar AP, Couldwell WT, Chen JC, et al. Predictive value of serum prolactin levels measured immediately after transsphenoidal surgery. *J Neurosurg*. 2002;97:307–314.
- Maric A, Kruljac I, Cerina V, et al. Endocrinological outcomes of pure endoscopic transsphenoidal surgery: a Croatian Referral Pituitary Center experience. *Croat Med J*. 2012;53:224–233.
- Tampourlou M, Trifanescu R, Paluzzi A, et al. Therapy of endocrine disease: surgery in microprolactinomas: effectiveness and risks based on contemporary literature. *Eur J Endocrinol*. 2016;175:R89–R96.
- Bartynski WS, Boardman JF, Grahovac SZ. The effect of MR contrast medium dose on pituitary gland enhancement, microlesion enhancement and pituitary gland-to-lesion contrast conspicuity. *Neuroradiology*. 2006; 48:449–459.
- Colao A, Boscaro M, Ferone D, et al. Managing Cushing's disease: the state of the art. *Endocrine*. 2014;47:9–20.
- Grober Y, Grober H, Wintermark M, et al. Comparison of MRI techniques for detecting microadenomas in Cushing's disease. *J Neurosurg*. 2018; 128:1051–1057.
- Vitale G, Tortora F, Baldelli R, et al. A.B.C. Group. Pituitary magnetic resonance imaging in Cushing's disease. *Endocrine*. 2017;55:691–696.
- Batista D, Courkoutsakis NA, Oldfield EH, et al. Detection of adrenocorticotropin-secreting pituitary adenomas by magnetic resonance imaging in children and adolescents with Cushing disease. *J Clin Endocrinol Metab*. 2005;90:5134–5140.
- Chowdhury IN, Sinaii N, Oldfield EH, et al. A change in pituitary magnetic resonance imaging protocol detects ACTH-secreting tumours in patients with previously negative results. *Clin Endocrinol (Oxf)*. 2010; 72:502–506.
- Kasaliwal R, Sankhe SS, Lila AR, et al. Volume interpolated 3D-spoiled gradient echo sequence is better than dynamic contrast spin echo sequence for MRI detection of corticotropin secreting pituitary microadenomas. *Clin Endocrinol (Oxf)*. 2013;78:825–830.
- Arnaldi G, Angeli A, Atkinson AB, et al. Diagnosis and complications of Cushing's syndrome: a consensus statement. *J Clin Endocrinol Metab*. 2003;88:5593–5602.
- Tabarin A, Laurent F, Catargi B, et al. Comparative evaluation of conventional and dynamic magnetic resonance imaging of the pituitary gland for the diagnosis of Cushing's disease. *Clin Endocrinol (Oxf)*. 1998; 49:293–300.
- Tins B, Cassar-Pullicino V, Haddaway M, et al. Three-dimensional sampling perfection with application-optimised contrasts using a different flip angle evolutions sequence for routine imaging of the spine: preliminary experience. *Br J Radiol*. 2012;85:e480–e489.
- Wu Y, Wang J, Yao Z, et al. Effective performance of contrast enhanced SPACE imaging in clearly depicting the margin of pituitary adenoma. *Pituitary*. 2015;18:480–486.
- Mihai G, Varghese J, Lu B, et al. Reproducibility of thoracic and abdominal aortic wall measurements with three-dimensional, variable flip angle (SPACE) MRI. *J Magn Reson Imaging*. 2015;41:202–212.
- Wang J, Wu Y, Yao Z, et al. Assessment of pituitary micro-lesions using 3D sampling perfection with application-optimized contrasts using different flip-angle evolutions. *Neuroradiology*. 2014; 56:1047–1053.
- Tang Y, Wu Y, Zhang H, et al. Increased diagnostic confidence in the diagnosis of pituitary micro-lesions with the addition of three-dimensional sampling perfection with application-optimized contrasts using different flip-angle evolutions sequences. *Acta Radiol*. 2019;60:213–220.
- Yi N, Ji L, Zhang Q, et al. Long-term follow-up of female prolactinoma patients at child-bearing age after transsphenoidal surgery. *Endocrine*. 2018;62:76–82.
- Melmed S, Casanueva FF, Hoffman AR, et al. Diagnosis and treatment of hyperprolactinemia: an Endocrine Society clinical practice guideline. *J Clin Endocrinol Metab*. 2011;96:273–288.
- Gillam MP, Molitch ME, Lombardi G, et al. Advances in the treatment of prolactinomas. *Endocr Rev*. 2006;27:485–534.
- Burlacu MC, Maiter D, Duprez T, et al. T2-weighted magnetic resonance imaging characterization of prolactinomas and association with their response to dopamine agonists. *Endocrine*. 2019;63:323–331.
- Zamanipoor Najafabadi AH, Zandbergen IM, de Vries F, et al. Surgery as a viable alternative first-line treatment for prolactinoma patients. A systematic review and meta-analysis. *J Clin Endocrinol Metab*. 2020; 105:e32–e41.
- Freda PU, Beckers AM, Katznelson L, et al. Pituitary incidentaloma: an endocrine society clinical practice guideline. *J Clin Endocrinol Metab*. 2011;96:894–904.
- Lasocki A, Caspersz L.J. T2-SPACE imaging of the cauda equina for the assessment of leptomeningeal metastatic disease. *J Clin Neurosci*. 2020; 81:290–294.
- Bapst B, Amegniz JL, Vignaud A, et al. Post-contrast 3D T1-weighted TSE MR sequences (SPACE, CUBE, VISTA/BRAINVIEW, isoFSE, 3D MVOX): technical aspects and clinical applications. *J Neuroradiol*. 2020; 47:358–368.
- Park HJ, Lee SY, Kang KA, et al. Comparison of two-dimensional fast spin echo T₂ weighted sequences and three-dimensional volume isotropic T₂ weighted fast spin echo (VISTA) MRI in the evaluation of triangular fibrocartilage of the wrist. *Br J Radiol*. 2018;91:20170604.

30. Park M, Lee SK, Choi J, et al. Differentiation between cystic pituitary adenomas and Rathke cleft cysts: a diagnostic model using MRI. *AJNR Am J Neuroradiol*. 2015;36:1866–1873.
31. Vilar L, Abucham J, Albuquerque JL, et al. Controversial issues in the management of hyperprolactinemia and prolactinomas—an overview by the Neuroendocrinology Department of the Brazilian Society of Endocrinology and Metabolism. *Arch Endocrinol Metab*. 2018;62:236–263.
32. Glezer A, Bronstein MD. Approach to the patient with persistent hyperprolactinemia and negative sellar imaging. *J Clin Endocrinol Metab*. 2012;97:2211–2216.
33. Wright K, Lee M, Escobar N, et al. Tumor volume improves preoperative differentiation of prolactinomas and nonfunctioning pituitary adenomas. *Endocrine*. 2021;74:138–145.
34. Mallea-Gil MS, Manavela M, Alfieri A, et al. Prolactinomas: evolution after menopause. *Arch Endocrinol Metab*. 2016;60:42–46.